Theor Chem Acc (2009) 123:317–325
DOI 10.1007/s00214-009-0551-y

REGULAR ARTICLE

Structural and electronic properties of small platinum metallorganic complexes

Giovanni Barcaro · Alessandro Fortunelli

Received: 26 November 2008 / Accepted: 23 February 2009 / Published online: 25 March 2009

Abstract A theoretical first-principles study of $Pt_n(ligand)_m$ ($n = 1$–3) metallorganic complexes is performed, by varying the number of metal atoms and the nature and number of organic coordinate ligands (specifically, vinylic and arylic ligands). For each system, the nature of the bonding, the structure and the energetics of the metal/organic-species interaction are analyzed to derive information on the growth of coated metal clusters in solution. It is found that two régimes can be distinguished: a "coordinatively saturated" régime, in which the ratio among the number of ligands and the number of metal atoms is high and a ligand/organic π-interaction mode is preferred, and a "coordinatively unsaturated" régime, in which the ligand/metal ratio is low and a ligand/organic σ-interaction mode is preferred. Reactive channels, such as oxidative insertion of Pt into C–H bonds with the corresponding formation of platinum hydride species, can be opened in the latter régime.

Keywords Density-functional theory · Metallorganic complex · Solvated metal clusters · σ-interaction · π-interaction

Dedicated to the memory of Professor Oriano Salvetti and published as part of the Salvetti Memorial Issue.

G. Barcaro (✉) · A. Fortunelli
Molecular Modeling Laboratory,
Istituto per i Processi Chimico-Fisici (IPCF) del Consiglio Nazionale delle Ricerche (CNR), Area della Ricerca,
Via G. Moruzzi 1, 56124 Pisa, Italy
e-mail: barcaro@ipcf.cnr.it

1 Introduction

Colloidal suspensions of transition metals are formed by metallic particles, ranging in size between 1 and 50 nm, which are stabilized by protective shells/layers to prevent coalescence phenomena [1–4]. The possibility of effectively stabilizing nanometric metallic particles with a high surface/volume ratio in solution allows for a quickly growing number of technological applications of such colloidal suspensions, in particular (but not exclusively) in the field of catalysis [5–10]. Bottom-up methods to produce these systems are based on the synthesis of metallic particles starting from elementary constituents, i.e., single atoms, ions, or small clusters. These methods primarily consist on the reduction of metal salts via chemical processes, the use of electrochemical techniques, the controlled decomposition of organometallic metastable compounds or the aggregation of metallic species in low oxidation state. A large number of stabilizing species, donor ligands, polymers and surfactants are used to control the growth of the freshly formed metallic particles and to protect the growing units from coalescence into the thermodynamic equilibrium phase: the bulk crystal [11–14].

In this context, the use of olefinic complexes of metals in a low oxidation state proves to be a clean route for obtaining colloidal suspensions of mono- and bi-metallic particles. In particular, the technique of metal vapor deposition [1, 2, 15] is based on the co-condensation of vapors of one metal and of one or more organic solvents on the cold walls (−196 °C) of proper reactors in ultra-high vacuum (10^{-4}–10^{-6} mbar). The subsequent heating of the reactor determines the melting of the solvent to give solutions in which small atoms or very minute metallic clusters (containing no more than 10 atoms, normally less than 4) are coated by the solvent molecules or added

surfactants. An inconvenience of this technique is represented by the low thermical stability of the solvates, which quite often, even if kept at low temperatures, decompose slowly with the formation of insoluble aggregates. This determines a variation both in the concentration of the metal in solution as well as in the size of the particles and, as a consequence, in the catalytic properties. A possible solution to stabilizing the solvates consists in using emulsifying species (such as long chain aliphatic ammines or olefinic systems) capable of coordinating the metallic atoms in order to prevent the coalescence of the aggregates.

Given the high affinity of Pt towards unsaturated organic compounds, ligands based on C=C functional groups have been devised and tested [16, 17]: using the metal vapor deposition technique, colloidal suspensions of platinum have been obtained in the presence of deuterated benzene (C_6D_6) as solvent species and molecules of vinylsiloxanic compounds as stabilizing species [18]. In more detail, the surfactants used were 1,3-divinyl-1,1,3,3-tetramethyldisiloxane (DVS) and 1,3,5,7-tetravinyl-1,3,5,7-tetramethyl-cyclotetrasiloxane (TVS), whose structures are shown in Fig. 1. For both these compounds, the interaction with platinum occurs through the terminal olefinic groups. Experimental evidence has shown that in the presence of only the solvent molecules the stability of these suspensions at room temperature is limited to a few days, while with the use of surfactants the stability of metal aggregates is extended to a few months. The effective mechanisms by which growth eventually takes place, however, are not known, and are difficult to investigate experimentally, due to the lack of proper characterization tools able to furnish information on reactive processes in situ and in real time. Computational approaches can provide a very useful support in this sense, as it is nowadays possible to explore the structure, energetics and dynamics of aggregates of reasonable size with sufficient accuracy, see for example [19], a field into which one of us (AF) was introduced by Prof. Salvetti many years ago.

In the present article, such an enterprise is undertaken in the specific case of neutral small Pt clusters interacting with surfactants in which the ligand is based on unsaturated organic groups. The lowest-energy structures of $Pt_n ligand_m$ complexes where $n = 1$–3, $m = 1$–6, and ligand is a vinylic or arylic species, have been investigated via density-functional (DF) calculations. Our aim is to elucidate the nature of the interaction, the structure of the solvated species and the energetics of the metal/ligand detachment. It will be shown that it is possible to derive from such studies information useful to interpret experimental observations and suggestions with some general significance.

The article is structured as follows. In Sect. 2, the computational details will be given; the results will be discussed in Sect. 3 and the conclusions will be summarized in Sect. 4.

2 Computational details

Density-functional (DF) calculations have been performed using the DFT module of the NWChem software [20], adopting the B3LYP xc-functional [21] for the description of the exchange-correlation energy. It is known that this functional does not provide an adequate description of the metal bond, especially when this is fully developed in large clusters [22]. However, here we are dealing with small Pt units, for which the B3LYP functional is still appropriate. Moreover, some calculations have also been performed by employing the BPW91 [23, 24] exchange-correlation functional. The differences between the two functionals will be discussed in the next section. The structural search was mostly carried out via biased (or inspired) guesses, i.e., by setting up reasonable initial configurations and locally minimizing their energy at the DF level. However, in selected cases, a few steps of a density-functional basin-hopping (DF-BH) approach were also performed. In the DF-BH approach [25, 26], one

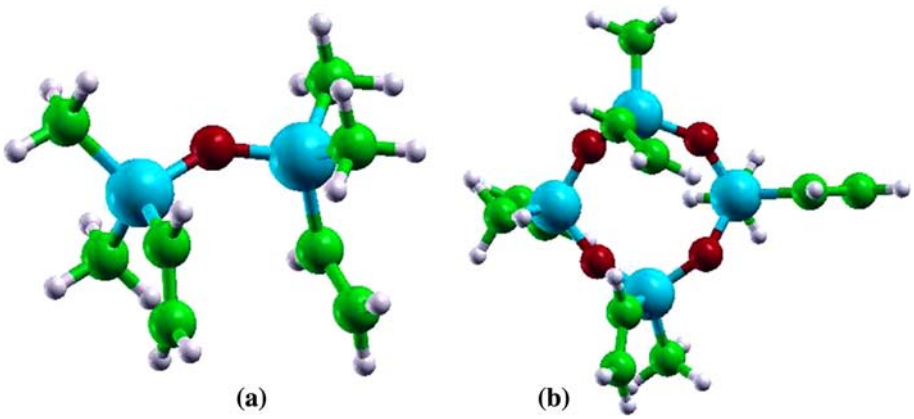

Fig. 1 **a** 1,3-divinyl-1,1,3,3-tetramethyldisiloxane (DVS) and **b** 1,3,5,7-tetravinyl-1,3,5,7-tetramethyl-cyclotetrasiloxane (TVS). Oxygens in *red*, carbons in *green*, hydrogens in *white* and silicons in *light blue*

starts from a random configuration and tries to explore the PES of the system by random moves followed by local minimizations whose acceptance is ruled by a Monte Carlo Metropolis criterion. Alternatively, one can start the DF-BH search from inspired guesses, in which selected plausible structures are set up and locally minimized, trying to exploit for the larger systems the experience acquired with small ones.

For the DF calculations, the chosen basis set included Gaussian functions of triple-ζ quality plus polarization functions (f on the platinum atom, d on the carbon, oxygen and silicon atoms and p on the hydrogen atom) [27, 28]. In the case of the platinum atom, a relativistic effective core potential (ECP) has been employed for the description of the 60 inner electrons [28]. All calculations have been performed spin-unrestricted and using a Gaussian-smearing technique [29] for the fractional occupation of the one-electron energy levels. The pictures have been obtained by using the XCrySDen program [30].

3 Results

Our aim is to elucidate the basic principles of the metal/ligand interaction from which models for the aggregation and coalescence of metal clusters can be developed. In the following, the results on $Pt_n(C_2H_4)_m$ complexes will be presented and discussed according to the number of Pt atoms in the complex.

3.1 $Pt_1(ligand)_m$

Before going further into the study of the structure of $Pt_n(ligand)_m$ complexes, it is useful to conduct a preliminary analysis of the Pt^0/C=C interaction (carbon–carbon double bond) in the simplest possible case: the interaction of one platinum atom with an ethylene molecule (C_2H_4), recalling some of the results obtained in [31]. In the gas phase, the electronic configuration of the platinum atom is a $5d^96s^1$ triplet state. When the Pt atom interacts with the ethylene molecule, there is a change from the $5d^96s^1$ triplet state to the $5d^{10}6s^0$ singlet state. In this transition the $6s$ platinum orbital is vacated, making it available for a *donation* of electron density from the organic species. The d orbitals, which now become completely filled and slightly more diffuse, are in turn available for *back-donating* electron density to the π^* orbitals of the double bond. This phenomenon is apparent in the density plots of the molecular orbitals of the $Pt(C_2H_4)$ complex shown in Fig. 2a–c. 0.5 eV are necessary to promote the Pt atom to its valence state (averaging spin–orbit contributions). Once the Pt atom is in its valence state, the formation of the chemical bond produces a significant amount of energy, 2.67 eV. Overall, the total variation of energy in the reaction:

$$Pt + C_2H_4 \rightarrow Pt(C_2H_4) \quad \Delta E = -2.17 \text{ eV} \tag{1}$$

is equal to 2.17 eV, see Table 1, where the results obtained on the energetics of small Pt systems are reported. When the platinum–ethylene distance is increased, one can observe a *spin-crossing* following bond breaking: the asymptotic state (with the two fragments at infinite distance) is characterized by a different spin from the bonding state.

The complex $Pt(C_2H_4)$ can bind a second and a third ethylene molecules, forming larger complexes, see Fig. 2d, e. In the final $Pt(C_2H_4)_3$ complex, approximately all of the carbon atoms lye in the same plane as the platinum atom. The bonding mechanism, with the interplay of the σ-donation and π-back-donation, is the same in the presence of a greater number of ethylene molecules, but the energy gains resulting from the addition of a second and third ligand molecule are smaller than that of the reaction (1)

$$Pt(C_2H_4) + (C_2H_4) \rightarrow Pt(C_2H_4)_2 \quad \Delta E = -1.36 \text{ eV} \tag{2}$$

$$Pt(C_2H_4)_2 + (C_2H_4) \rightarrow Pt(C_2H_4)_3 \quad \Delta E = -0.74 \text{ eV} \tag{3}$$

These interaction energies are approximately the same when the ethylene molecules are substituted by ligands with vinylic terminal groups, as in the case of the three complexes shown in Fig. 2f–h, where 1,3-divinyl-1,1,3,3-tetramethyldisiloxane (DVS) is the ligand species. The energies of the corresponding reactions are

$$Pt + DVS \rightarrow Pt(DVS)^{[2f]} \quad \Delta E = -2.16 \text{ eV} \tag{4}$$

$$Pt(DVS)^{[2f]} \rightarrow Pt(DVS_{chelate})^{[2g]} \quad \Delta E = -1.39 \text{ eV} \tag{5}$$

$$Pt(DVS_{chelate})^{[2g]} + DVS \rightarrow Pt(DVS_{chelate})(DVS)^{[2h]} \quad \Delta E = -0.65 \text{ eV} \tag{6}$$

This leads us to conclude that ethylene molecules are good models of ligands with vinylic terminals with a significant reduction of the computational cost. Note that the only significant difference is between Eqs. 3 and 6 is due to the steric effects.

In order to complete this preliminary analysis, we have calculated the dissociative barrier corresponding to the detachment of one of the three vinylic groups of the $Pt(DVS)_2$ complex, more specifically the detachment of the DVS non-chelated species, that is, bonded to platinum via just one vinylic group. The energy curve was obtained by progressively increasing the distance from the center of mass of the exiting vinylic part and the platinum atom. With this distance kept at a fixed value, a local optimization of all the other degrees of freedom of the system was carried out for every point. The obtained curve (not

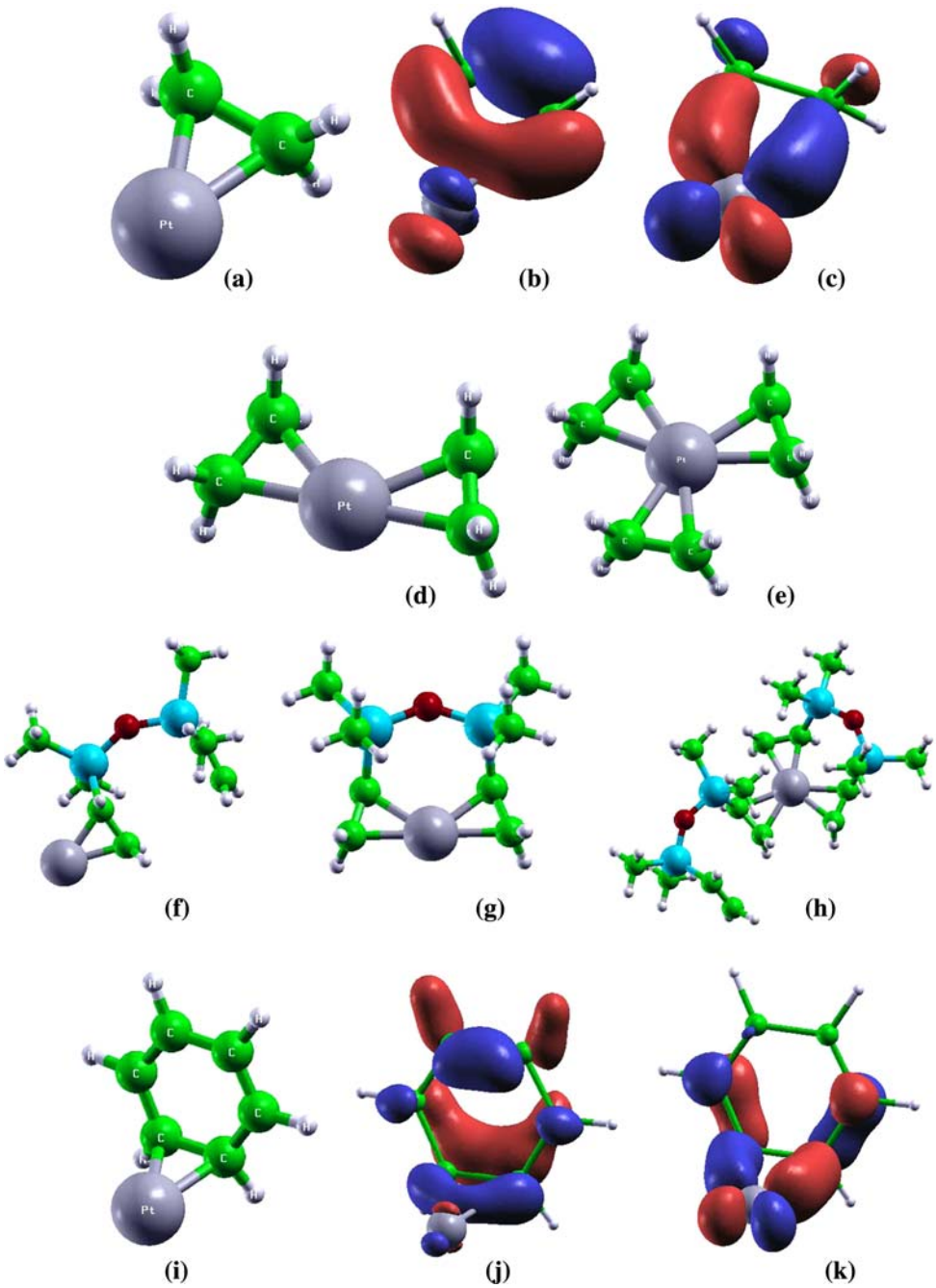

Fig. 2 **a** Structure of the $Pt(C_2H_4)$ complex and **b**, **c** two of its molecular orbitals; **b** donation process from the π orbitals of the organic species to a $d-s$ hybrid orbital of the metal; **c** back-donation process from the metal orbitals to the π^* orbitals. The two isosurfaces correspond to a density value of 0.07 a.u. Structure of the complexes (**d**) $Pt(C_2H_4)_2$, **e** $Pt(C_2H_4)_3$, **f** Pt(DVS) with only one C=C bond interacting, **g** Pt(DVS) with both C=C bonds interacting, and **h** $Pt(DVS)_2$. **i** Structure of the $Pt(C_6H_6)$ complex and **j**, **k** two of its molecular orbitals highlighting the **j** donation and **k** back-donation processes. *Color coding* as in Fig. 1, with platinums in *dark grey*

reported) shows that fragmentation of the complex occurs without any additional energy barrier with respect to the energy loss of the Pt/vinyl bond. As this barrier is not large (0.65 eV), this process is predicted to be already active at room or at a slightly higher temperature. The experimental evidence shows that solutions containing vinylic surfactants are stable for a time-span of some months at room temperature, but for much shorter periods even with minimal heating. This suggests that, once platinum becomes coordinately unsaturated (i.e., it loses a ligand), it can aggregate with other unsaturated species present in the solution, thus causing a progressive growth of the metal cluster. Once it reaches a critical size, growth accelerates, causing a precipitation of the metal aggregate, and consequently an instability of the solution.

The question that arises at this point is whether the detached DVS ligand is substituted by one of the surrounding solvent molecules (benzene or deuterated benzene). In such a case, platinum would not be in a coordinatively unsaturated state, therefore hindering the growth of the metal aggregate. A first hint to answer this question comes from the fact that if in the CVD process the

Table 1 Energetic analysis of the Pt/ligand interaction in the case of vinylic and arylic organic species

Complex	Binding energy (eV)
$Pt + C_2H_4$	2.17
$Pt + C_6H_6$	1.73
$Pt(C_2H_4) + C_2H_4$	1.36
$Pt(C_2H_4) + C_6H_6$	0.80
$Pt(C_6H_6) + C_2H_4$	1.71
$Pt(C_6H_6) + C_6H_6$	1.04
$Pt(C_2H_4)_2 + C_2H_4$	0.74
$Pt(C_2H_4)_2 + C_6H_6$	≤ 0
$Pt(C_6H_6)_2 + C_2H_4$	≤ 0
$Pt(C_6H_6)_2 + C_6H_6$	≤ 0

co-condensation of the metal vapors happens in the presence of the solvent vapors only (without any surfactant), the solution thus obtained is stable for a time span of few days, indicating that the interaction with the solvent molecules is much weaker than that with surfactants. To shed some light on this point, we carried out a study of the interaction of platinum atoms also with arylic organic ligands. The first system looked at was the Pt/benzene complex, see Fig. 2i–k. Figure 2j, k shows that the interaction between metal and organic part is very similar to the platinum/ethylene case with the major difference that the bond energetics is greatly reduced by the need of breaking the aromatic system and to localize the π electrons of benzene [32]. Benzene is thus a much weaker ligand than ethylene (see Table 1)

$$Pt + C_6H_6 \rightarrow Pt(C_6H_6) \quad \Delta E = -1.23 \text{ eV} \tag{7}$$

Mesethylene, $C_6H_3(CH_3)_3$, often used as a solvent, behaves in a completely analogous way with an almost identical reaction energy

$$Pt + C_6H_3(CH_3)_3 \rightarrow Pt(C_6H_3(CH_3)_3) \quad \Delta E = -1.21 \text{ eV} \tag{8}$$

The weakness of the Pt/aryl bonding is further confirmed by the addition of a second and third benzene in order to complete the coordination of the platinum atom, in analogy to what observed in the case of vinylic ligands. The second benzene binds with an interaction energy of 1.04 eV, while the third benzene does not bind to the complex. The latter fact is significant in view of the growth process in solution because it means that in the presence of an arylic solvent, or even an arylic surfactant, a complete saturation of the platinum coordination valence is not reached, thus allowing the growth of the metal cluster even at room temperature. The same behavior occurs when platinum is coordinated to vinylic groups and a benzene group attempts to attach itself: a benzene molecule binds to the $Pt(C_2H_4)$ complex with an interaction energy of 0.80 eV, but is not able to bind to the $Pt(C_2H_4)_2$ complex. This shows that in the case of the fragmentation of the $Pt(DVS)_2$ complex considered above, once platinum is in a coordinatively unsaturated state due to the loss of a surfactant molecule, an arylic solvent molecule (benzene or mesethylene) cannot replace the vinylic ligand and block the coordination of the metal: the only event that can take place is the addition of another fragment leading to the formation of a Pt–Pt bond and the consequent growth of the metallic aggregate. Eventhough the DF approach does not take into account dispersion interactions, the absence of covalent bonding implies small energy barriers for the opening of the Pt coordination shell.

3.2 $\mathbf{Pt_2(ligand)_m}$

In the gas-phase, Pt_2 is a triplet: the 5*d* and 6*s* orbitals are hybridized leading to the formation of a strong σ-bond. At the B3LYP level, the Pt-Pt bond energy is estimated to be 2.15 eV (bond distance of 2.53 Å). Note that at the BPW91 level, which is a better functional to describe neutral Pt clusters, the bond energy rises to 3.24 eV (close to the experimental value of 3.15 eV [33, 34]) and the bond length decreases to 2.37 Å. Nevertheless, as we will see, these quantitative differences do not seem to qualitatively affect the interaction of the metal cluster with the organic ligands.

In the case of the interaction with a single ethylene molecule, two different configurations can be obtained: the first, shown in Fig. 3a–c, is similar to the one observed for the single platinum atom (π-interaction mode) and is characterized by a σ-donation/π-back-donation interaction. For Pt_2, however, the Pt/ethylene interaction is much weaker (1.62 eV instead of 2.67 eV) and the formation of the bond is not accompanied by any spin-crossing (the spin state of the final complex is still a triplet): this is mainly due to the tendency of the system to optimize the metal–metal interaction at the expense of the weaker metal–ligand interaction. The second configuration (σ-interaction mode), shown in Fig. 3d–f, results more stable than the former by about 0.7 eV. In this configuration, the two platinum atoms form real σ-bonds with the two carbon atoms. This process is accompanied by a shortening of the Pt–C distances with respect to the π-configuration (2.02 Å instead of 2.16 Å) and a corresponding elongation of the C–C distance in the organic ligand (from 1.40 to 1.51 Å) due to the fact that the double bond basically becomes a single bond. A deeper analysis reveals that the carbon atoms are now sp^3 hybridized with a tetrahedral disposition of the H atoms around the carbons. The coupling of the unpaired *d* electrons of the two platinum atoms with the carbons valence electrons makes that the spin state of this complex is zero (singlet state) and thus implies that Pt_2 is in a valence state

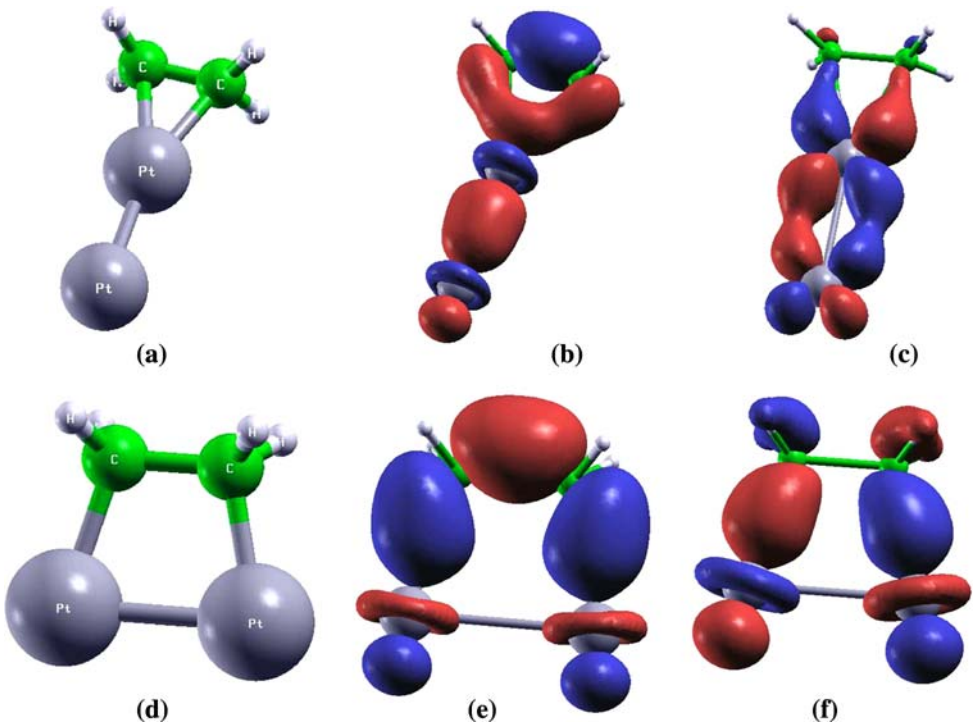

Fig. 3 **a–c** π-configuration of the $Pt_2(C_2H_4)$ complex (total spin S = 0) and two of its molecular orbitals, where the mechanism of **b** donation and **c** back-donation is clarified. **d–f** σ-configuration of the $Pt_2(C_2H_4)$ complex (total spin S = 1) and two of its molecular orbitals, where it is shown how the donation/back-donation mechanisms are accompanied by the formation of σ-bonds among platinum and carbon atoms. *Color coding* as in Fig. 2

(d^{10}–d^{10}) that can be estimated to be at least 1 eV higher in energy than the triplet ground state [34]. The interaction of the ethylene molecule with the dimer is indeed stronger than in the previous case (2.32 eV = 1.62 eV + 0.70 eV). These results were obtained employing the B3LYP xc-functional. By repeating the calculation with the BPW91 functional, the greater strength of the Pt–Pt bond makes that the interaction with the organic molecule is weaker. In fact the σ-configuration (interaction energy of 2.20 eV) is still favored over the π-configuration (interaction energy of 1.74 eV), but by only 0.46 eV, determining a quantitative but not a qualitative difference among the two approaches. An analysis of the molecular orbitals (MO) of the resulting complexes highlights the electronic differences between σ- and π-interaction modes. In the π-configuration (Fig. 3b, c) the situation is similar to that found in the case of a single Pt atom: Fig. 3b shows the σ-donation and Fig. 3c shows the π-back-donation mechanisms. In contrast, the MO plots of the σ-configuration show that the orbitals consist of a symmetric (Fig. 3e) and anti-symmetric (Fig. 3f) combinations of true (although distorted) Pt–C covalent bonds.

In the case of the interaction of the platinum dimer with two ethylene molecules, several configurations can be realized. The most significant are those shown in Fig. 4a–d. All of them are characterized by a zero net value of the total spin, thus implying a promotion of 1 eV to the valence state of the dimer. In the case of Fig. 4a, a double π-configuration takes place; by pairing the unpaired *d* electrons, the system sacrifices part of the metallic bond to better interact with the organic species: this is reflected in the elongation of the Pt–Pt distance (from 2.53 to 2.78 Å). The interaction of the $Pt_2(C_2H_4)$ complex with the second ethylene molecule is strongly decreased (0.57 eV instead of 1.62 eV), but this decrease is also due to the spin-crossing energy penalty. Among the four configurations shown, the lowest in energy is Fig. 4b, where we observe a copresence of a σ- and a π-configuration. The ethylene in the π-configuration interacts with 1.12 eV, this value being decreased by the presence of the first group in σ-configuration. Also in this case, the functional BPW91 does not lead to any qualitative changes of the described results, as shown by the numbers in parentheses in Fig. 4. It is interesting to observe that, starting from the lowest energy configuration of the species $Pt_2(C_2H_4)$, the addition of the second organic group takes place in π-configuration, whereas the formation of a second σ-configuration is higher in energy by 0.77 eV.

For the complex $Pt_2(C_2H_4)_3$, as shown in Fig. 4e–g, the third organic molecule adds to the lowest configuration of the previous complex via a π-configuration. In general, this addition determines a global decrease of the σ character of the interaction in favor of the π-interaction; this is due to the fact that the π-configuration is characterized by a more delocalized character and is thus favored in the case of a larger number of ligands. These considerations also hold in the case of the complex $Pt_2(C_2H_4)_4$, see Fig. 4h, i, where the interaction of the dimer with the four ligands in the lowest-energy structure (4*h*) takes place only through π-configurations.

It is important to note that in this case the configuration in which all the four (C_2H_4) units interact in the

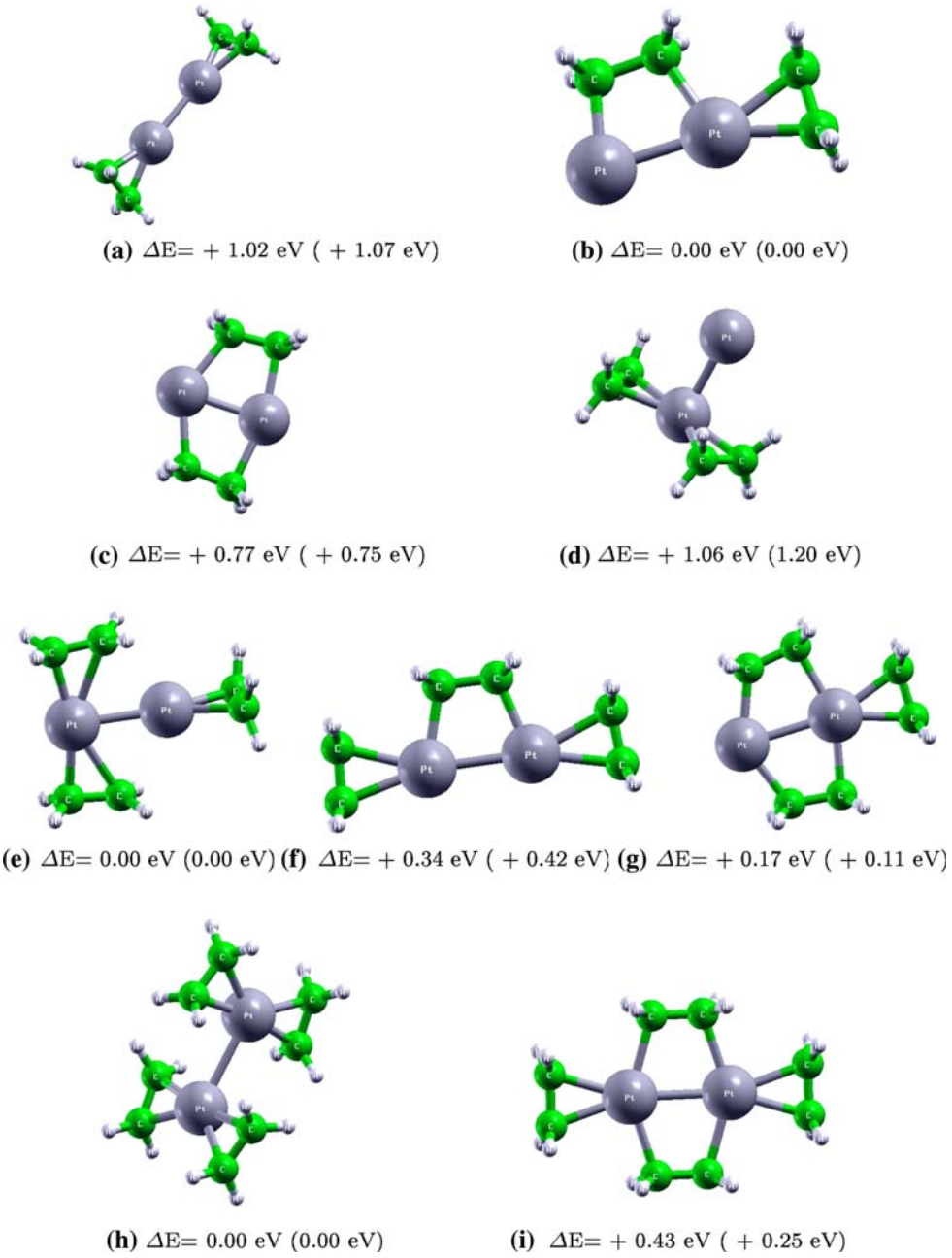

Fig. 4 **a–d** Configurations of the $Pt_2(C_2H_4)_2$ complex; **e–g** configurations of the $Pt_2(C_2H_4)_3$ complex; **h**, **i** configurations of the $Pt_2(C_2H_4)_4$ complex. For each structure, the relative energy is indicated at the B3LYP level and, in parenthesis, at the BPW91 level. The total spin is S = 0 for all the configurations shown. *Color coding* as in Fig. 2

π-configuration mode is favored with respect to the one in which two of the (C_2H_4) molecules interact in the σ-configuration mode. A *transition* from σ-configuration to π-configuration thus occurs as a function of the number of ligands. We can translate this finding into information useful for studying the growth process by distinguishing two régimes: a "coordinatively saturated" régime, in which the ratio among the number of ligands molecule and the number of metal atoms is high, and a "coordinatively unsaturated" régime, when this ratio is low. Our calculations imply that the π-interaction mode is energetically favored in the coordinatively saturated régime, whereas the σ-interaction mode is favored in the coordinatively unsaturated régime.

3.3 $\mathbf{Pt_3(ligand)}_m$

The putative global minimum of the $Pt_3(C_2H_4)_6$ complex is shown in Fig. 5a. By comparison with other σ-interacting configurations (not shown), it is confirmed that σ-interaction is disfavored when the number of coordinating (C_2H_4) units is high. The average interaction energy of each ethylene molecule with the Pt trimer is now 0.92 eV (for a total ΔE of 5.52 eV). Figure 5b, c show another

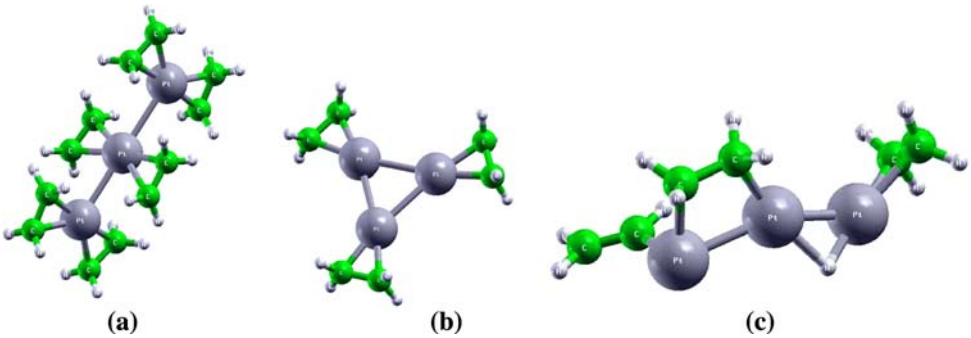

Fig. 5 **a** Putative global minimum of the $Pt_3(C_2H_4)_6$ complex; **b** π-configuration of the $Pt_3(C_2H_4)_3$ complex; **c** insertion of a Pt in the C–H bond to give an hydride complex. At the B3LYP level, **c** is lower in energy by 0.33 eV with respect to **b**. The total spin is S = 0 for all the configurations shown. *Color coding* as in Fig. 2

interesting effect. Figure 5b represents the lowest-energy configuration of the complex $Pt_3(C_2H_4)_3$ obtained imposing the π-coordination mode, with an average interaction energy of each ethylene molecule with the Pt trimer in the triangular configuration of 0.51 eV (for a total ΔE of 1.53 eV). If, however, one relaxes this geometrical constraint and performs a few steps of a DF-BH algorithm, the structure of Fig. 5c results. It can be noted that Fig. 5c corresponds to the oxidative insertion of Pt into a C–H bond, and, at the B3LYP level, is lower in energy by 0.33 eV with respect to the Fig. 5b. We can thus predict that in the coordinatively unsaturated régime, reactive channels can be opened, with the formation of Pt hydrides. This rationalizes the experimental NMR observation of signals in the hydride regions especially in non-controlled surfactant-poor conditions [17, 35]. It can also be noted that the total spin for all the configurations shown in Fig. 5 is S = 0: again, the interation with the ligands promotes the Pt cluster to a valence state in which the local spin is quenched (the ground state of the Pt trimer is a triangular triplet, even though a triangular singlet is only 0.03 eV higher in energy, while the linear arrangement has S = 2 and is 1.04 eV higher in energy with respect to the ground state [34]).

4 Conclusions

In this work, a theoretical first-principles study of the $Pt_n(ligand)_m$ ($n = 1, 3$) metallorganic complexes has been performed, by varying the number of metal atoms and the nature and number of organic coordinate ligands (specifically, vinylic and arylic ligands). From the analysis of the results, several conclusions can be drawn.

First of all, ethylene has been shown to be a good model (at least, at the electronic level) for the vinylic functional groups of the DVS ligand. Clearly, the *steric* properties are different: in the case of DVS, steric hindrance can disfavor the achievement of full coordination thus favoring growth or, on the opposite, can impose constraints on reactive processes.

Second, the Pt/carbon–carbon double bond interaction has a many-body character, i.e., the binding energy appreciably decreases with the number of interacting C=C units.

Third, aromatic species are much weaker ligands than vinylic species, due to the need of disrupting π-electron conjugation. This fact, coupled with the many-body character of the Pt/ligand interaction, makes that a third aromatic molecule does not bind to a doubly coordinated Pt center, thus leaving it free for further aggregation.

Fourth, the many-body character of the Pt/ligand interaction also makes that the detachment energy barriers of a fully coordinated Pt center are not high, and can be overcome at room or slightly higher temperatures.

Fifth, when considering metal dimers or larger clusters, there exist two metal/organic binding mechanisms: one involving the formation of σ bonds between Pt and C atoms (σ-interaction mode) and one in which the metal/ligand interaction takes place through a donation/back-donation mechanism (π-interaction mode). The latter mechanism is the only one occurring for a single Pt atom. It can be noted that the need to locally vacate the Pt *s* orbitals in the π-interaction mode or to make this orbital available to covalent bonding in the π-interaction mode, entails a promotion of the Pt atom to a valence "interaction" state with a corresponding quenching of the local spin. This promotion, which for small clusters corresponds to a weakening of the metal–metal bonds, has an energy cost that must be taken into account when evaluating or predicting the Pt/ligand binding energy or parametrizing Pt/ligand empirical potentials, and represent the metal analogue of the preparation of the fragments in the interacting state discussed in [36].

Sixth, two régimes can be distinguished: a "coordinatively saturated" régime, in which the ratio among the number of ligands and the number of metal atoms is high and the ligand/organic π-interaction mode is preferred, and a "coordinatively unsaturated" régime, in which this ratio is low and the ligand/organic σ-interaction mode is preferred. The coordinative unsaturation typical of the latter régime favors more complicated, reactive processes, such as oxidative insertion of Pt atoms into a C–H bond.

These conclusions are in tune with available experimental data, and suggest a positive role of theoretical simulations in the study of the nuclation and growth of metal clusters in the homogeneous phase in terms of accurate prediction of the energetics and of the kinetic growth parameters.

Acknowledgments We acknowledge financial support from the Italian CNR for the program "(Supra-) Self-Assemblies of Transition Metal Nanoclusters" within the framework of the ESF EUROCORES SONS, and from the European Community Sixth Framework Project for the STREP Project "Growth and Supra-Organization of Transition and Noble Metal Nanoclusters" (contract no. NMP-CT-2004-001594).

References

1. Klabunde KJ (1994) Free atoms, clusters and nanoscale particles. Academic Press, San Diego
2. Bradley JS (1994) Clusters and colloids. Wiley, Wienheim
3. Bonnemann H, Richards RM (2001) Eur J Inorg Chem 2455
4. Pileni MP (2003) C R Chimie 6:965
5. Schmid G (1996) Applied homogeneous catalysis with organometallic compounds, vol 2. Wiley, Wienheim, pp 636–644
6. Herrmann WA, Cornils B (1996) Applied homogeneous catalysis with organometallic compounds, vol 2. Wiley, Wienheim, pp 1171–1172
7. Bonnemann H, Brijoux W (1996) Advanced catalysts and nanostructured materials, chap 7. Academic Press, San Diego, pp 165–196
8. Schmidt TJ, Noeske M, Gasteiger HA, Behm RJ, Britz P, Brijoux W, Bonnemann H (1997) Langmuir 13:2591
9. Gotz M, Wendt H (1998) Electrochim Acta 43:3637
10. Schmidt TJ, Noeske M, Gasteiger HA, Behm RJ, Britz P, Bonnemann H (1998) J Electrochem Soc 145:925
11. Faraday M (1857) Philos Trans R Soc Lond 147:145
12. Aiken III JD, Finke RG (1999) J Mol Catal A 145:1
13. Toshima N, Yonezawa T (1998) New J Chem 22:1179
14. Leisner T, Rosche C, Wolf S, Granzer F, Woste L (1996) Surf Rev Lett 3:1105
15. Blackborrow JR, Young D (1979) Metal vapor synthesis. Springer, New York
16. Hitchcock PB, Lappert MF, Warhurst NJW (1991) Ang Chem Int Ed 30:438
17. Uccello-Barretta G, Balzano F, Evangelisti C, Raffa P, Mandoli A, Nazzi S, Vitulli G (2008) J Organomet Chem 693:1276
18. Lewis LN, Colborn RE, Grade H, Bryant GL, Sumpter CA, Scott RA (1995) Organometallics 14:2202
19. Ciacchi LC, Pompe W, DeVita A (2001) J Am Chem Soc 123:7371
20. Kendall RA, Aprà E, Bernholdt DE, Bylaska EJ, Dupuis M, Fann GI, Harrison RJ, Ju J, Nichols JA, Nieplocha J, Straatsma TP, Windus TL, Wong AT (2000) Comput Phys Commun 128:260
21. Becke AD (1993) J Chem Phys 98:1372
22. Aprá E, Fortunelli A (2000) J Mol Struct/Theochem 501–502:251
23. Becke AD (1988) Phys Rev A 38:3098
24. Perdew JP, Chevary JA, Vosko SH, Jackson KA, Pederson MR, Singh DJ, Fiolhais C (1992) Phys Rev B 46:6671
25. Aprà E, Ferrando R, Fortunelli A (2006) Phys Rev B 73:205414
26. Barcaro G, Aprà E, Fortunelli A (2007) Chem Eur J 13:6408
27. Schaefer A, Huber C, Ahlrichs R (1994) J Chem Phys 100:5829
28. Andrae D, Haussermann U, Dolg M, Stoll H, Preuss H (1990) Theor Chim Acta 77:123
29. Elsasser C, Fahnle M, Chan CT, Ho KM (1994) Phys Rev B 49:13975
30. Kokalj A (1999) J Graph Model 17:176
31. Fortunelli A, Velasco AM (2002) J Mol Struct/Theochem 586:17
32. Roszak S, Balasubramanian K (1995) Chem Phys Lett 234:101
33. Taylor S, Lemire GW, Hamrick YM, Fu ZW, Morse MD (1988) J Chem Phys 89:5517
34. Fortunelli A (1999) J Mol Struct/Theochem 493:233
35. Evangelisti C, Raffa P, Balzano F, Uccello-Barretta G, Vitulli G, Salvadori P (2008) J Nanosci Nanotech 8:2096
36. Carter EA, Koel BE (1990) Surf Sci 226:339